ARTICLE

A Homozygous Mutation in Human *PRICKLE1* Causes an Autosomal-Recessive Progressive Myoclonus Epilepsy-Ataxia Syndrome

Alexander G. Bassuk,[1,2,3] Robyn H. Wallace,[7] Aimee Buhr,[2] Andrew R. Buller,[1] Zaid Afawi,[8] Masahito Shimojo,[9] Shingo Miyata,[10] Shan Chen,[1] Pedro Gonzalez-Alegre,[4] Hilary L. Griesbach,[5] Shu Wu,[1] Marcus Nashelsky,[6] Eszter K. Vladar,[11,12] Dragana Antic,[11,12] Polly J. Ferguson,[1] Sebahattin Cirak,[16] Thomas Voit,[17] Matthew P. Scott,[12,13,14,15] Jeffrey D. Axelrod,[11] Christina Gurnett,[18] Azhar S. Daoud,[19] Sara Kivity,[20] Miriam Y. Neufeld,[8] Aziz Mazarib,[22] Rachel Straussberg,[21] Simri Walid,[23] Amos D. Korczyn,[24] Diane C. Slusarski,[5] Samuel F. Berkovic,[25,*] and Hatem I. El-Shanti[1,2,26]

Progressive myoclonus epilepsy (PME) is a syndrome characterized by myoclonic seizures (lightning-like jerks), generalized convulsive seizures, and varying degrees of neurological decline, especially ataxia and dementia. Previously, we characterized three pedigrees of individuals with PME and ataxia, where either clinical features or linkage mapping excluded known PME loci. This report identifies a mutation in *PRICKLE1* (also known as *RILP* for REST/NRSF interacting LIM domain protein) in all three of these pedigrees. The identified *PRICKLE1* mutation blocks the PRICKLE1 and REST interaction in vitro and disrupts the normal function of PRICKLE1 in an in vivo zebrafish overexpression system. PRICKLE1 is expressed in brain regions implicated in epilepsy and ataxia in mice and humans, and, to our knowledge, is the first molecule in the noncanonical WNT signaling pathway to be directly implicated in human epilepsy.

Introduction

More than a dozen clinico-molecular forms of progressive myoclonus epilepsy (PME) are known, including Unverricht-Lundborg disease (MIM 254800 resulting from *CSTB* mutations [MIM 601145]), Lafora disease (MIM 254780 resulting from *EPM2A* [MIM 607566] or *NHLRC1* [MIM 608072] mutations), the family of neuronal ceroid lipofuscinoses (with a variety of molecular defects including *PPT1* [MIM 256730], *CLN4* [MIM 204300], and *CLN5* [MIM 256731] mutations), and myoclonic epilepsy with ragged red fibers (MERFF [MIM 545000] with mitochondrial t-RNA mutations). Previously, we characterized three families with individuals affected with PME and ataxia but normal brain imaging, where either clinical features or linkage mapping excluded known PME loci.[1–3]

This report identifies a mutation in *PRICKLE1* (MIM 608500) in all three of these pedigrees. PRICKLE1 is part of the noncanonical or planar cell polarity (WNT/PCP) pathway, in which some WNT family members activate a β-CATENIN (*CTNNB1* [MIM 116806])-independent pathway.[4] In *Drosophila* and vertebrates, the WNT/PCP pathway likely regulates cell polarization.[5] Depleting *Prickle* genes in the zebrafish embryo alters the convergent-extension movements essential for gastrulation and disrupts normal calcium signaling.[6–8] *PRICKLE1* is part of a gene family encoding proteins containing a highly conserved PET domain, which mediates Prickle1-protein-binding interactions.[6,9–11] Prickle1 was discovered independently based on its ability to bind and functionally interact with the *RE1-SILENCING TRANSCRIPTION FACTOR* (*REST* [MIM 600571], which was thus separately named Rilp, for REST/NRSF interacting LIM domain protein), an essential regulator of neural genes.[12,13] The *PRICKLE1* mutation identified in this study is located in the PET domain and disrupts the PRICKLE1 and REST interaction in vitro and alters the normal function of PRICKLE1 in an in vivo zebrafish overexpression system.

[1]Department of Pediatrics, [2]Graduate Program in Genetics, [3]Graduate Program in Neuroscience, [4]Department of Neurology, [5]Department of Biology, [6]Department of Pathology, University of Iowa, Iowa City, IA 52242, USA; [7]Queensland Brain Institute, The University of Queensland, Brisbane 4072, Australia; [8]Department of Neurology, Tel Aviv Sourasky Medical Center and Sackler Faculty of Medicine, Tel Aviv University, Tel Aviv 64239, Israel; [9]Department of Molecular and Cellular Biochemistry, University of Kentucky, Louisville, KY 40536, USA; [10]Department of Anatomy & Neuroscience, Graduate School of Medicine, Osaka University, Osaka 565-0871, Japan; [11]Department of Pathology, [12]Department of Developmental Biology, [13]Department of Genetics, [14]Department of Bioengineering, [15]Howard Hughes Medical Institute, Stanford University School of Medicine, Stanford, CA 94305, USA; [16]Universitätskinderklinik Essen, Abteilung für Allgemeine Pädiatrie mit Schwerpunkt Neuropädiatrie, 45122 Essen, Germany; [17]Institut de Myologie Groupe Hospitalier Pitié-Salpêtrière, 75013 Paris, France; [18]Department of Neurology, Division Pediatric Neurology, Washington University School of Medicine, St. Louis, MO 63110, USA; [19]Department of Pediatrics, Jordan University of Science and Technology, Irbid 22110, Jordan; [20]Epilepsy Unit, [21]Department of Child Neurology, Schneider Children's Medical Center of Israel, Petach Tikvah 49202, Israel; [22]Kupat Holim Clalit, Nazareth 16000, Israel; [23]Department of Neurology, Western Galilee Hospital, Nahariya 22100, Israel; [24]Sieratzki Chair of Neurology, Tel Aviv University, Ramat Aviv 69978, Israel; [25]Epilepsy Research Centre and Department of Medicine, University of Melbourne (Austin Health), Heidelberg West, Victoria 3161, Australia; [26]Shafallah Medical Genetics Center, Doha, Qatar
*Correspondence: s.berkovic@unimelb.edu.au
DOI 10.1016/j.ajhg.2008.10.003.

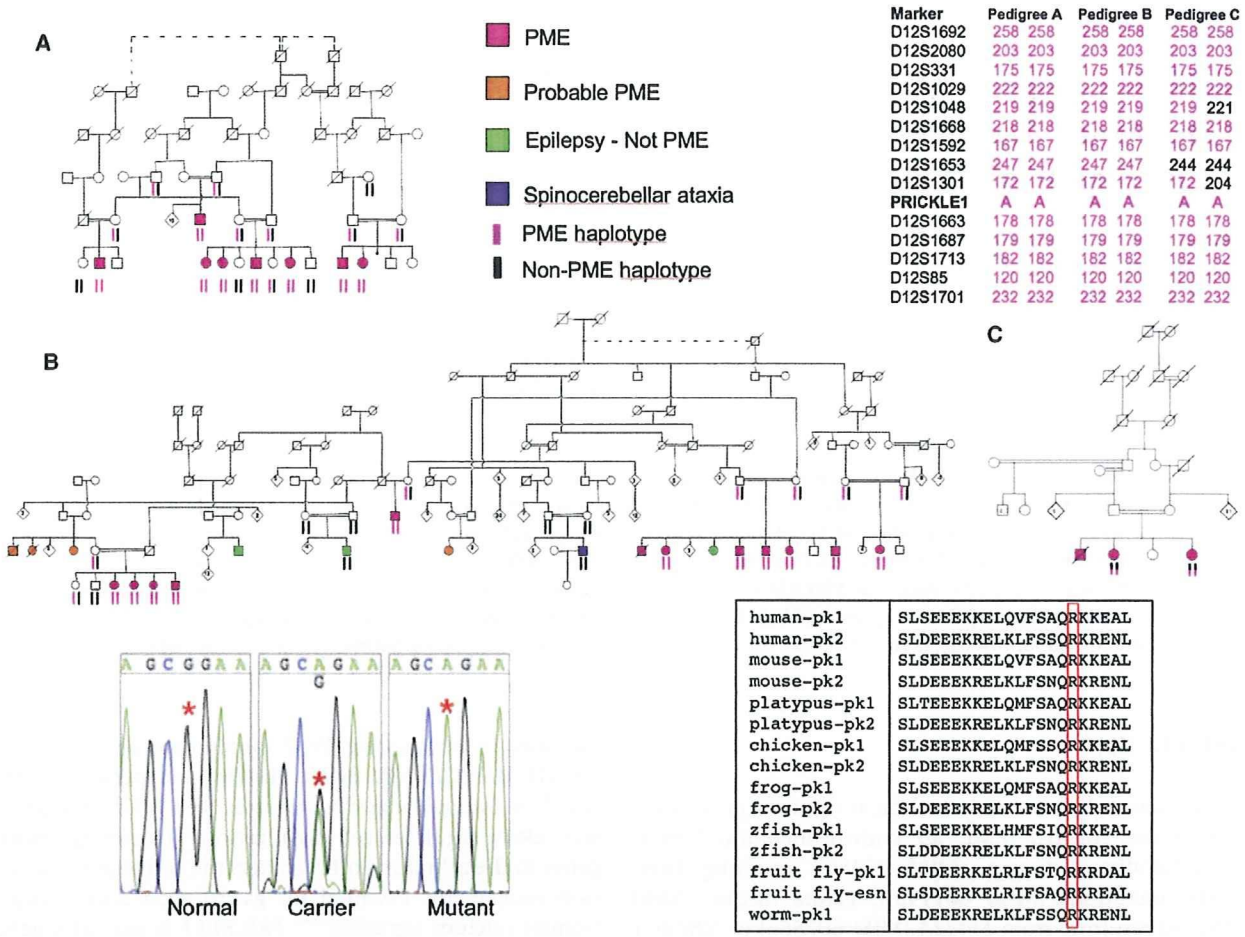

Marker	Pedigree A	Pedigree B	Pedigree C
D12S1692	258 258	258 258	258 258
D12S2080	203 203	203 203	203 203
D12S331	175 175	175 175	175 175
D12S1029	222 222	222 222	222 222
D12S1048	219 219	219 219	219 221
D12S1668	218 218	218 218	218 218
D12S1592	167 167	167 167	167 167
D12S1653	247 247	247 247	244 244
D12S1301	172 172	172 172	172 204
PRICKLE1	A A	A A	A A
D12S1663	178 178	178 178	178 178
D12S1687	179 179	179 179	179 179
D12S1713	182 182	182 182	182 182
D12S85	120 120	120 120	120 120
D12S1701	232 232	232 232	232 232

human-pk1	SLSEEEKKELQVFSAQRKKEAL
human-pk2	SLDEEEKRELKLFSSQRKRENL
mouse-pk1	SLSEEEKKELQVFSAQRKKEAL
mouse-pk2	SLDEEEKRELKLFSNQRKRENL
platypus-pk1	SLTEEEKKELQMFSAQRKKEAL
platypus-pk2	SLDEEEKRELKLFSNQRKRENL
chicken-pk1	SLSEEEKKELQMFSSQRKKEAL
chicken-pk2	SLDEEEKRELKLFSNQRKRENL
frog-pk1	SLSEEEKKELQMFSAQRKKEAL
frog-pk2	SLDEEEKRELKLFSNQRKRENL
zfish-pk1	SLSEEEKKELHMFSIQRKKEAL
zfish-pk2	SLDDEEKRELKLFSNQRKRENL
fruit fly-pk1	SLTDEERKELRLFSTQRKRDAL
fruit fly-esn	SLSDEERKELRIFSAQRKREAL
worm-pk1	SLDEEEKRELKLFSSQRKRENL

Figure 1. Pedigrees of the Affected Families, Representative Sequences, and Evolutionary Comparison of the Altered PRICKLE1 Amino Acid

Nine nuclear families from three pedigrees including 23 subjects with progressive myoclonus epilepsy and ataxia (pink symbol). Boxes on pedigrees indicate individuals previously reported by Berkovic et al.[1] (A), El-Shanti et al.[2] (B), and Straussberg et al.[3] (C). Dotted lines indicate individuals believed to be related, but the exact relationship was unknown. Subjects who probably had the familial syndrome but were not personally examined are shown in orange. Shared chromosome 12 haplotypes of affected subjects are shown on the top right. Haplotypes were remarkably stable within nuclear families and extended pedigrees. Individuals with epilepsy or ataxia, clinically distinct from the familial syndrome (green and purple symbols), did not share the haplotypes or have the *PRICKLE1* mutation. Representative DNA sequence chromograms from normal, carrier, and affected (mutant) individuals are in the bottom left panel with the red asterisks denoting the position of the abnormal nucleotide. Amino acid sequence alignment surrounding the altered amino acid for PRICKLE proteins in multiple species. pk1, Prickle1 protein; pk2, Prickle2 protein; esn, espinas protein; zfish, zebrafish. Accession numbers for the protein sequences are: human-pk1, NP_694571; human-pk2, NP_942559; mouse-pk1, NP_001028389; mouse-pk2, NP_001074615; platypus-pk1, XP_001505284; platypus-pk2, XP_001508261; chicken-pk1, XP_416036; chicken-pk2, XP_001234704; frog-pk1, NP_001016939; frog-pk-2, NP_001103517; zfish-pk1, NP_899185; zfish-pk2, NP_899186; fruit fly-pk1, NP_724534; fruit fly-esn, CAB64381; worm-pk1, NP_741435. The amino acid altered in the families and the corresponding amino acid in Prickle proteins from other species are boxed in red.

Material and Methods

Subjects

Clinical details of the three pedigrees were previously described;[1–3] pedigree B was subsequently expanded with eight more affecteds identified in three nuclear families. Clinical studies were approved by the Institutional Review Boards of the Tel Aviv Sourasky Medical Center and the Jordan University of Science and Technology. Informed consent was obtained from participating subjects and their legal guardians. The control brain specimens were obtained from a 60-year-old male with cirrhosis who died suddenly of atherosclerotic heart disease, after exemption by the Institutional Review Board of the University of Iowa and within guidelines established by Iowa statute.

Fine Mapping and Haplotyping

Microsatellite markers within the chromosome 12 pericentromeric linkage region were selected from the Marshfield human linkage map. Genotyping of 47 individuals from 3 families (Figure 1) was performed by the Australian Genome Research Facility. Marker order is based on the current human sequence map (NCBI Build 36.3).

Resequencing

PRICKLE1 amplicons (Table S2 available online) were sequenced with an automated ABI sequencer with dye terminator chemistry. After DNA amplification, unincorporated PCR primers and dNTPs in the sample were removed prior to sequencing by isolation of the desired band in a 2% agarose gel, followed by column purification. Sequences were analyzed with the computer program PHRED, which calls the bases, and PHRAP that assembled the sequence on a PC.

Control Genotyping

The 1054 individuals from the HGD-CEPH panel and the 300 Middle Eastern individuals were genotyped with the Taqman (ABI) assay on an ABI 7900 HT Fast Real Time PCR machine with the following primers according to manufacturer's instructions: PR1ex4-ex4F, GAAAAAAGAGTTGCAGGTGTTCAGT; PR1ex4-ex4R, TTAAT TGTTCCTCTTCCCAGTGCTT; PR1ex4-ex4V1, VIC, CTCAGCGGA AGAAA; PR1ex4-ex4M1, FAM, CTCAGCAGAAGAAA.

The entire *PRICKLE1* gene was also directly resequenced in an additional 288 individuals, including 96 individuals of Jordanian-Palestinian ancestry.

Immunohistochemistry and Immunostaining Protocols

For mouse sections and HeLa cells, the solution used was PBS 1× Dulbecco's (pH 7.4) and the blocking solution for rabbit antibodies used was serum-free blocking media (Dako, X0909). For mouse combined with rabbit antibodies, we used M.O.M. Mouse Ig Blocking Reagent (Vector, BMK-2202); add 2 drops of stock solution to 2.5 ml of PBS. For human sections, the solution used was PBS 1X Dulbecco's (pH 7.4) and the blocking solution was serum-free blocking media (Dako, X0909).

Antibodies

Rabbit polyclonal antibody to mouse Prickle1 was produced with amino acids 808–822 by A.G.B. and with amino acids 339–514 by D.A. Specificity for Prickle1 and not Prickle2 was confirmed by immunostaining of myc-tagged cDNAs encoding Prickle1 or Prickle2 proteins into HeLa cells (data not shown). NeuN (Chemicon), GFAP (Dako), myc 9E10 (Sigma), and GFAP (Santa Cruz) antibodies were used at a 1:400–1:500 dilutions for immunohistochemistry and immunoblotting. Mouse and rabbit antibodies were diluted in M.O.M. Diluent (600 μl of protein concentrate stock solution added to 7.5 ml of PBS [Vector, BMK-2202]). Sequential rabbit antibodies were diluted in PBS 1X. Secondary antibodies were diluted 1/500 in blocking for mouse+rabbit antibodies or in PBS for rabbit antibody. We used the goat anti-rabbit IgG $(Fab')_2$-Alexa Fluor 568 conjugated antibody (Invitrogen, A21069) for the anti-GFAP antibody and the goat anti-mouse IgG $(Fab')_2$-Alexa Fluor 568 conjugated Ab (Invitrogen, A11019) for anti-NeuN antibody. We used the goat anti-rabbit IgG $(Fab')_2$-Alexa Fluor 488 conjugated Ab (Invitrogen, A11070) for the Prickle1 antibodies. The nuclear counterstain To-Pro3 (Invitrogen, T3605) was diluted 1/2000 in PBS 1X or DAPI. Slides were mounted with Vector Labs, H-1000.

Staining Protocol, Mouse Sections

Procedure. Procedures were performed at room temperature or as indicated. Sections were deparaffinized with autostainer program #3 and rehydrated with ddH_2O. To perform antigen retrieval by microwave, citrate buffer (pH 6.0) was prewarmed for ~30 s in a Teflon Coplin jar, and slides were added under the following conditions: restriction temperature, +95°C; wattage, #6 (601 W); pulse 5 min, hold 5 min (no microwave applied), pulse 5 min, then slides were left in the dish to cool to room temperature for about 20 min. Next, slides were washed in PBS 1X (pH 7.4), 3x3 min. Sections were permeabilized with 0.1% Triton X-100 in PBS for 10 min, washed in PBS 1X (pH 7.4), 3x3 min. Blocking was performed for rabbit and mouse primary antibodies together by applying the working solution of M.O.M. mouse Ig blocking reagent X1 hr, then PBS 3x3 min, then working solution M.O.M. diluent for 5 min.

Primary Antibodies. Serum-free blocking media was added for 1 hr, then primary antibodies were added at the following dilutions: rabbit anti-prickle 1 antibodies 1/250-1/375 were added with mouse anti-NeuN (Chemicon, MA13377) 1/500 or rabbit anti-prickle 1 affinity-purified antibody 1/250-1/375 was added followed by rabbit anti-GFAP Ab (Dako, Z0344) 1/1000 and stored in a slide folder at +4°C.

Sequential Stainings. The following variation was used. Sections were blocked (serum-free protein block) for 30 min, then primary antibody (anti-GFAP antibody) was added for 1 hr, then washed with PBS 1X (pH 7.4), 6 times for 3 min, and then the secondary antibody-conjugated fluorophore was added (in the dark) for 30 min. The slide was then washed with PBS 1X (pH 7.4), 6x for 3 min. Nuclear counterstain (in the dark) was then added for 5 min. Slides were then rinsed in PBS 1X and mounted in VectaShield and stored in slide-folder at +4°C. Nuclei were viewed in the Far red channel (647 nm Ex). Anti-Prickle1 antibodies were viewed in the green channel (488 nm Ex), and anti-GFAP or anti-NeuN antibodies were viewed in red channel (568 nm Ex).

Staining Protocol, Human Sections

Procedure. Procedures were performed at room temperature or as indicated. Sections were deparaffinized (with an autostainer) and rehydrated with ddH_2O. Antigen retrieval was performed by microwave staining. Citrate buffer (pH 6.0) was prewarmed in the microwave for ~30 s in a Teflon Coplin jar. Slides were then added with temperature restriction: +95°C, wattage: #6 (601 W), pulse 5 min, hold 5 min (no microwave applied), pulse 5 min. Slides were then cooled to room temperature for about 20 min, washed in PBS 1X (pH 7.4), 3x for 3 min, and permeabilized with 0.1% Triton X-100 in PBS for 10 min, washed in PBS 1X (pH 7.4), 3x3 min blocked with serum-free blocking media for 1 hr. Primary antibodies were added for 1 hr, then washed with PBS, 6x for 3 min, secondary antibodies were added in the dark for 1 hr, then washed with PBS, 6x for 3 min. Slides were mounted with VectaShield and sections were stored in a slide folder at +4°C.

Primary Antibodies. Primary antibodies were diluted in PBS 1X. Rabbit anti-prickle 1 antibody 1/250-1/375 and mouse anti-NeuN (Chemicon, MA13377) 1/500 were used together, and rabbit anti-prickle 1 antibody 1/250-1/375 and rabbit anti-GFAP Ab (Dako, Z0344) 1/1000 were used sequentially. Goat anti-rabbit IgG $(Fab')_2$-Alexa Fluor 488 conjugated antibody (Invitrogen, A11070) secondary antibody was diluted 1/500 in PBS. To-Pro3 (Invitrogen, T3605) was diluted 1/2000 in PBS 1X and was used as the nuclear counterstain. Slides were mounted with VectaShield (Vector Labs, H-1000).

Sequential Stainings. After the first primary and secondary antibodies were applied, slides were blocked (serum-free protein block) for 30 min, and then the second primary antibody was applied for 1 hr, then the slides were washed in PBS 1X (pH 7.4), 6x for 3 min, and then the second secondary antibody-fluorophore conjugated was added in the dark for 30 min, and then washed in PBS 1X (pH 7.4), 6x for 3 min. Nuclear counterstain was then added (in the dark) for 5 min, and slides were rinsed with PBS

1X, and mounted in VectaShieldand and stored in a slide-folder at +4°C. Nuclei are viewed in the far red channel (647 nm Ex), anti-Prickle1 antibodies are viewed in the green channel (488 nm Ex), and anti-NeuN or GFAP antibodies are viewed in red channel (568 nm Ex).

HeLa Cell Staining

Mouse monoclonal anti-Myc 9E10 (Sigma) 1/1000 was added (EGFP viewed directly in green channel), then PBS was added 6 times for 3 min followed by secondary antibodies in the dark for 1 hr, then PBS 6 times for 3 min, and slides were then mounted with VectaShield and double labeled sections were stored with Ms + Rb Abs in slide folder at +4°C.

Confocal Microscopy

All confocal microscopy was performed on a Zeiss 510 Confocal Microscope at the University of Iowa or on a Leica confocal microscope at Stanford University. The thickness of the confocal images and all details of exposure time are embedded within the digital photographs used in this manuscript and available upon request.

Plasmids

The full-length human *PRICKLE1* cDNA in the PCR-bluntII-TOPO (Open Biosystems) was cloned into the EcoRI (5′) and XhoI (3′) sites of the pCS2+ vector, with the EGFP epitope added in-frame to the 3′ end of the gene by PCR site-directed mutagensis/chimeragnesis. The R104Q encoding mutation was introduced by site-directed mutagenesis, and the entire cDNA was resequenced after introduction of the mutation to insure that no additional mutations were introduced. Myc-REST was the same construct used previously to define the Prickle-REST interaction.[12,13]

Transfections

Transfections into HeLa cells were performed as previously described.[12,13]

Nuclear REST Measurement. To measure the impact of the PRICKLE1 mutation on the localization of REST, cells transfected with wild-type and myc-REST or mutant PRICKLE1 and myc-REST and quantified with a variation of the method previously reported.[14,15] All GFP+/myc+ cells were counted and a score of 4 was assigned for myc nuclear fluorescence much greater than myc cytoplasmic fluorescence, 3 for myc nuclear fluorescence greater than myc cytoplasmic fluorescence, 2 for myc nuclear fluorescence equal to myc cytoplasmic fluorescence, 1 for myc nuclear fluorescence less than myc cytoplasmic fluorescence, and 0 for myc nuclear fluorescence much less than myc cytoplasmic fluorescence. The mean REST nuclear score was calculated for 100 GFP+/myc+ cells in each condition.

Coimmunoprecipitations

Coimmunoprecipitations with slight variations as previously described.[12,13] In brief, myc-mouse REST and GFP-human Prickle1 plasmids were cotransfected into HeLa cells according to the Lipofectamine 2000 protocol. After 48 hr incubation, cells were lysed with 300 μl cold NET-N + Roche Protease Inhibitor. Lysates were sonicated 3 times for 4 s. 60 μl of the crude lysates were removed and mixed with 110 μl of denaturing loading buffer. The remaining lysates were precleared by adding 5 μl of anti-rabbit beads and rotating at room temperature for 20 min. The beads were removed by centrifuging samples briefly at 10,000 rpm and removing the supernatant. Precleared lysates were then mixed with 10 μl rabbit anti-GFP conjugated beads (Santa Cruz) and rotated for 2 hr at 4°C, followed by 30 min rotation at room temperature. The supernatant was removed and the beads rinsed 3 times with 500 μL of cold NET-N lysis buffer. After rinsing, 80 μl of denaturing loading buffer was added to the immunoprecipitated samples. 15 μl of IP lysates or 10 μl of crude lysates were loaded onto a 10% SDS-PAGE gel, ran for 75 min at 200V, and electroblotted overnight at 140 mA. Membrane was incubated 1:2000 anti-GFP (Roche) or anti-myc (Sigma) for 4 hr at 4°C.

PCR Conditions for Sequencing

Primers used are listed in Table S2. For exons 2–8, the mix used for PCR was: 2 μl DNA at 20 ng/μl, 2 μl 10× NH_4 reaction buffer, 2 μl dNTP (5 mM), 0.75 μl $MgCl_2$ (50 mM), 0.2 μl Biolase Taq (5 μm/μl), 0.5 μl forward primer, 0.5 μl reverse primer (20 μM per primer), add DDH2O to 20 μl. For exon 1, Invitrogen Platinum Pfx DNA polymerase was used. PCR cycling began after 10 min at 94°C as follows: (94°C, 45 s; annealing temperature, 30 s, 72°C, 45 s) ×35 cycles, followed by 72°C for 8 min, then 4°C until removed from thermocycler.

Zebrafish Constructs and Analysis

Zebrafish prickle cDNAs and wild-type and mutant (R → Q) PCR products were cloned into the Gateway vector system (Invitrogen). Both myc-tagged and untagged forms were created. Synthetic RNA was made with the mMessage machine kit (Ambion) and injected at the 1–8 cell stage. Alterations to gastrulation movements were monitored by live image capture at 20 hr postfertilization and older. Additionally, embryos were fixed at the 8–10 somite stage for whole-mount in situ hybridization with the molecular marker *MyoD*, which labels the midline as well as the developing somites. Equivalent protein expression was verified by myc-immunostaining and western blotting.

Statistical Analysis

The results of the zebrafish injections were subjected to the Fisher's exact test with the following contingency numbers: wild-type Zfsh pk1: 6 normal embryos, 36 defective embryos; mutant Zfish pk1: 20 normal embryos, 30 defective embryos; total: 26 normal embryos, 66 defective embryos.

Results

We analyzed disease features and genetics in three consanguineous Middle-Eastern pedigrees with autosomal-recessive progressive myoclonic epilepsy syndromes with ataxia[1–3] that most closely resembled Unverricht-Lundborg disease, but without mutations in *CSTB*. Pedigree A (Figure 1) from Northern Israel was originally reported as progressive myoclonus epilepsy (a new form of Unverricht-Lundborg disease; *EPM1B*) beginning between 5 and 10 years; individuals were seen in adolescence or adult life and difficulty walking prior to onset of myoclonus was reported but not directly observed.[1] Part of pedigree B was seen in Jordan when subjects were young and the impressive feature was an early-onset ataxia with later myoclonus and seizures.[2] Re-evaluation subsequently showed features of progressive myoclonus epilepsy that was also present in newly identified members of this pedigree residing in Jordan and Northern Israel. Similarly, pedigree C was initially

regarded as a predominant ataxic syndrome when children were examined in the first decade, but later re-examination showed florid progressive myoclonic epilepsy.[3] The three affected children had impaired upgaze that was also observed in some affected members of pedigrees A and B. Features of a mild sensory neuropathy seen in pedigree C were not seen in the other families.

In all three pedigrees, comprising nine nuclear families, ataxia began at 4 to 5 years and evolved into an unequivocal PME phenotype with ataxia. In many forms of PME, cognitive decline is severe and generally occurs early; however, in this disorder intellect is usually preserved. Furthermore, in all affected individuals tested, brain magnetic resonance imaging gave unremarkable results. Table 1 summarizes the clinical and molecular features compared to Unverricht-Lundborg disease.

Previous linkage analysis mapped the disease locus in pedigree A and part of pedigree B (Figure 1) to the pericentromeric region of chromosome 12.[1,2] Pedigree B was next expanded considerably, and in all three pedigrees, haplotype analysis of microsatellite markers showed an identical haplotype over 12 Mb in pedigrees A and B, whereas pedigree C shared only the distal 250,000 base pairs with pedigrees A and B (Figure 1). Pedigrees A and B shared the same family name and were thought to be distantly related but the relationship could not be established with genealogical information for 5–6 generations. Pedigree C resided in a different village, had a different family name, and elders denied a connection to the family name of pedigrees A and B and to their villages.

Resequencing the entire coding region and intron-exon boundries of 47 genes in the original linkage region (Tables S1 and S2) revealed a single, shared, missense-nucleotide change in the coding region of *PRICKLE1* in all three families (c.311G → A [R104Q]; Figure 1, bottom left). The altered amino acid in PRICKLE1 lies within the highly conserved PET domain and is invariant in evolution from humans to worms and in the related PRICKLE2 and *Drosophila* Espinas proteins (Figure 1, bottom right). This nucleotide change segregated with the clinical phenotype in all three pedigrees and was neither present in any of 1054 individuals from the CEPH-HGD control DNA samples,[16] nor found in 300 samples from unrelated Middle-Eastern individuals without epilepsy. Resequencing the entire *PRICKLE1* coding region showed no other variants in another 288 control individuals without PME (including 96 Middle-Eastern individuals).

Taken together, the high degree of conservation of the residue affected by the missense change, the absence of the identified nucleotide change in more than 1300 controls (2600 chromosomes), and the lack of other PRICKLE1 variants in nearly 300 additional controls strongly support that the *PRICKLE1* gene mutation causes this autosomal-recessive, progressive myoclonus epilepsy-ataxia syndrome.

Prickle1 is expressed in multiple brain regions throughout mouse embryonic development, including regions implicated in epilepsy such as the hippocampus, cerebral cortex, and thalamus, as well as the primitive cerebellum[17–20] (and data not shown). We performed immunohistochemical analysis with two different Prickle1-specific antibodies, each directed against a distinct epitope. In this way we also detected Prickle1 expression in the postnatal murine thalamus, hippocampus, cerebral cortex, and cerebellum (Figure 2). Costaining these tissues with the neuron-specific marker NeuN and the glia-specific marker GFAP demonstrated that Prickle1 is specifically expressed in neurons, but not in glia (Figures 2C, 2D, 2G, 2H, 2K, and 2L; cerebellum costaining not shown). Similarly, in human adult thalamus, hippocampus, cerebral cortex, and cerebellum, PRICKLE1 is in neurons rather than glia (Figure 3; GFAP staining not shown). These findings demonstrate that PRICKLE1 is expressed in multiple areas of the brain thought to be involved in generating seizures (neurons of thalamus, hippocampus, and cerebral cortex) and ataxia (cerebellar neurons).

To evaluate the functional effect of this mutation on PRICKLE1-partner protein interactions, we tested whether mutant PRICKLE1 can coimmunoprecipitate REST (Figure 4). Although, as previously described, wild-type PRICKLE1 binds REST directly,[12,13] mutant PRICKLE1 fails to bind REST in vitro. Furthermore, because REST nuclear localization is altered in brains from patients with Huntington's disease with known mutations in Huntingtin,[21] we tested whether mutant PRICKLE1 affected the subcellular localization of REST. Indeed, in HeLa cells, immunolocalization shows that whereas overexpression of wild-type PRICKLE1 results in cytoplasmic retention of REST, overexpressed mutant PRICKLE1 fails to retain REST in the cytoplasm (representative cells are shown in Figure 5A). To quantify the effect of mutant PRICKLE1 on REST nuclear localization, we counted cells based on REST expression in the cytoplasm, nucleus, or both cytoplasm and nucleus, in cells cotransfected with REST+PRICKLE1 versus REST + mutant PRICKLE1 and found significantly increased nuclear REST in cells cotransfected with mutant PRICKLE1 (Figure 5B). Therefore, the identified *PRICKLE1* mutation

Table 1. Comparison of the Progressive Myoclonus Epilepsy-Ataxia Syndrome Described Here to Classical Unverricht-Lundborg Disease

	Progresssive Myoclonus Epilepsy-Ataxia Syndrome	Unverricht-Lundborg Disease[a]
First symptom	ataxia around age 4 yr	myoclonic or tonic-clonic seizures
Seizure onset: mean	7 yr	10–11 yr
Seizure onset: range	5–10 yr	6–16 yr
Progressive features	worsening myoclonus, ataxia, impaired up-gaze	worsening myoclonus, ataxia
Cognitive decline	mild or absent	mild or absent
Mode of inheritance	autosomal recessive	autosomal recessive
Linkage	12p11–q13	21q22.3
Gene	*PRICKLE1*	*Cystatin B*

[a] Modified and updated from Berkovic et al.[1]

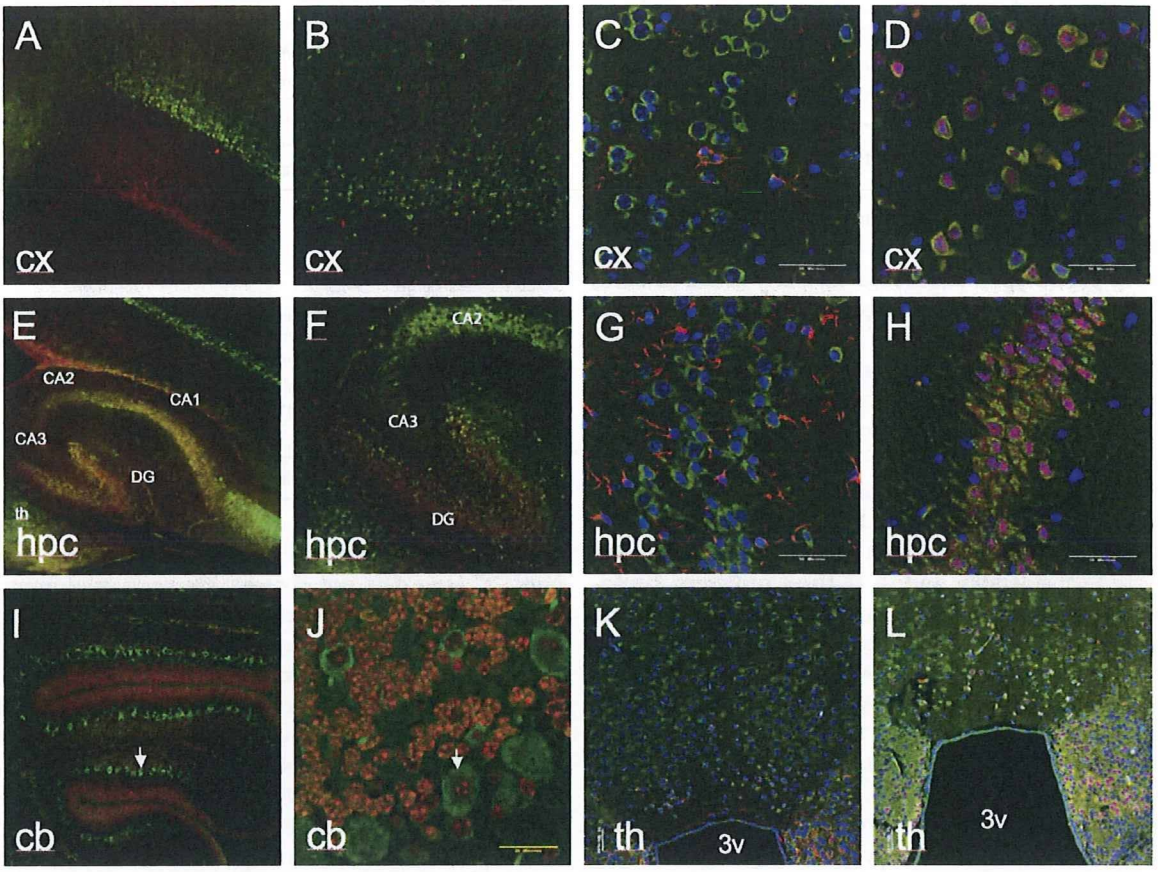

Figure 2. Expression of Prickle1 in Postnatal Mouse Brain

Prickle1 expression in cortex (A–D), hippocampus (E–H), cerebellum (I, J), and thalamus (K, L). For (A), (B), (E), (F), (I), and (J), Prickle1 antibody, raised against epitope corresponding to amino acids 339–514 of Prickle1, is labeled with green secondary, nuclear staining is in red. For (C), (D), (G), (H), (K), and (L), Prickle1 antibody, raised against epitope corresponding to amino acids 808–822 of Prickle1, is labeled in green. In (C), (D), (G), (H), (K), and (L), nuclear staining is in blue. In (C), (G), and (K), GFAP staining is in red. In (D), (H), and (L), NeuN, staining is in red. Arrows point to representative cerebellar Purkinje cells. 3v, third ventricle from coronal section; CA1, CA2, CA3, hippocampal *Cornu Ammonis* subregions; cb, cerebellum; cx, cerebral cortex; DG, dentate gyrus; hpc, hippocampus; th, thalamus. Magnification is 10× in (A), (E), and (I); 20× in (B), (F), (J), (K), and (L); 60× in (C), (D), (G), and (H). (A), (B), (E), (F), (I), and (J) are from P7 brain, (C), (D), (G), (H), (K), and (L) are from adult brain. (A)–(J) are from sagittal sections, (K) and (L) are coronal sections. A representative sample of sagittal sections from a P19 brain at multiple magnifications can be found in Figure S1.

disrupts both normal REST-binding and REST subcellular localization.

To investigate whether the mutant Prickle1 protein is functionally different from the wild-type in vivo, we injected zebrafish embryos with RNA encoding either wild-type or mutant zebrafish *prickle1*. As previously demonstrated, overexpressing wild-type *prickle1* alters gastrulation, resulting in a reduced anterior-posterior length (Figures 6A and 6B) and lateral expansion of somites (Figures 6C and 6D). Here, we further demonstrated that, compared to wild-type Prickle1, expressing similar levels of R104Q mutant Prickle1 showed a significantly less pronounced phenotype (Figure 6E). Thus in a zebrafish overexpression assay, the identified *PRICKLE1* mutation alters the in vivo function of Prickle1.

Discussion

The finding of a shared haplotype and identical PRICKLE1 mutation in three separately ascertained families of the same ethnic group with PME suggests a founder effect. The variation reported in the original three reports is explained by the differences in ages of the subjects ascertained in the earlier studies. Longitudinal assessment showed a uniform phenotype summarized in Table 1. The genealogical data and smaller ancestral haplotype found in family C suggests that this family separated earlier from the common ancestral line.

The identification of a *PRICKLE1* mutation causing this PME-ataxia syndrome raises several issues regarding the biology of PRICKLE1 and the pathophysiology of

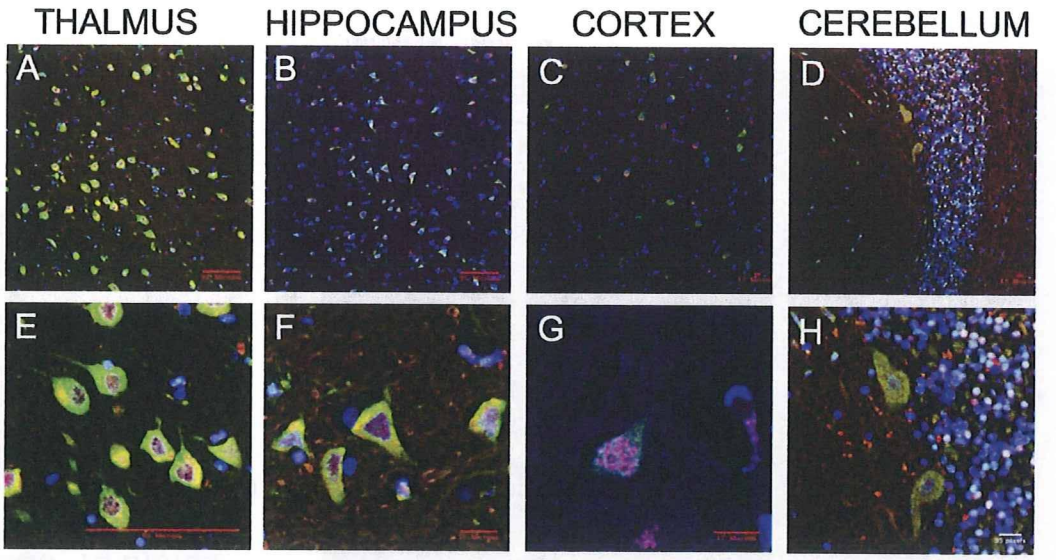

Figure 3. Expression of PRICKLE1 in Adult Human Brain
Low-power (A–D) and high-power (E–H) confocal images from immunostaining of adult human thalamus (A, E), hippocampus (B, F), cerebral cortex (C, G), and cerebellum (D, H). PRICKLE1 staining is in green, NeuN is in red, and nuclear staining is in blue. Scale markers are represented on the bottom right corner of each image.

neurological disease in these affected individuals. PRICKLE1 is part of the noncanonical or planar cell polarity (WNT/PCP) signaling pathway. In vivo studies in developing flies, frogs, and fish clearly demonstrated that Prickle1 is important for planar polarity signaling. Recently, mice lacking *Prickle1* were shown to die early in gestation, confirming an essential role for Prickle1 in development (H. Tao et al., 2008, Jap. Soc. Dev. Biol., abstract). At least some PRICKLE1 functions seem to be present in protein with the R104Q mutation because the mutation does not affect PRICKLE1 protein expression nor subcellular localization (Figure 5) and it still retains some wild-type function in our zebrafish overexpression system (Figure 6).

Our in vitro studies suggest that PRICKLE1 normally binds and translocates REST to the cytoplasm, thereby preventing REST from silencing target genes. The R104Q PRICKLE1 mutation lies within a known protein binding domain and thus disrupts REST binding (Figure 4), blocking the normal transport of REST out of the nucleus (Figure 5). These results suggest that tissues expressing mutant PRICKLE1 contain constitutively active REST which inappropriately downregulates REST target genes. This is significant because in addition to silencing neuronal genes in nonneuronal cells and neuronal precursors, REST also regulates target genes in mature neurons.[22] REST targets include ion channels and neurotransmitters, and the PME-ataxia syndrome may occur when brain regions expressing mutant PRICKLE1 misexpress these target genes. Although Prickle function was implicated in the control of cell division and morphogenesis during zebrafish neurulation[23] and REST activity was recently described in fish and frogs,[24] a role for the PRICKLE/REST interaction during neurogenesis has not yet been studied.

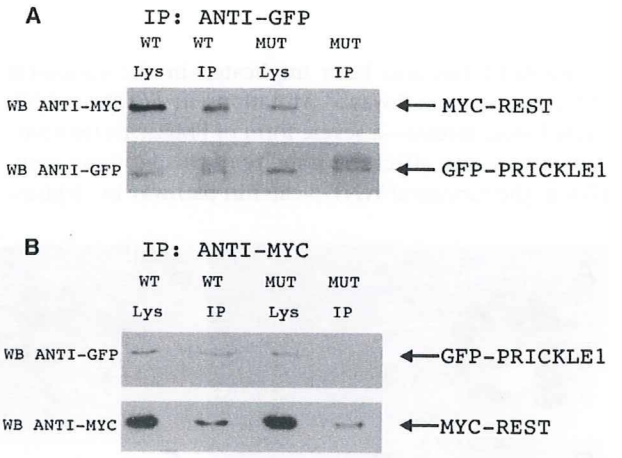

Figure 4. R104Q Mutant PRICKLE1 Has Impaired NRSF/REST Binding
Coimmunoprecipitation of REST with wild-type (WT) or R104Q mutant (MUT) encoding PRICKLE1 demonstrates decreased REST binding for MUT PRICKLE1. MYC-REST and either GFP-tagged WT or R104Q MUT PRICKLE1 plasmids were transfected into HeLa cells. Cell lysates were prepared in RIPA buffer and immunoprecipitated with agarose-conjugated anti-GFP antibody (A) or anti-MYC antibody (B). Immunoprecipitates (IP) were subjected to SDS-PAGE followed by western blotting (WB) with MYC or GFP antibodies. WB antibody noted to left of gels. The input (1/5) of immunoprecipitation is shown in the "Lys" lanes. Arrows to the right of the gels note the position of MYC-REST and GFP-PRICKLE1.

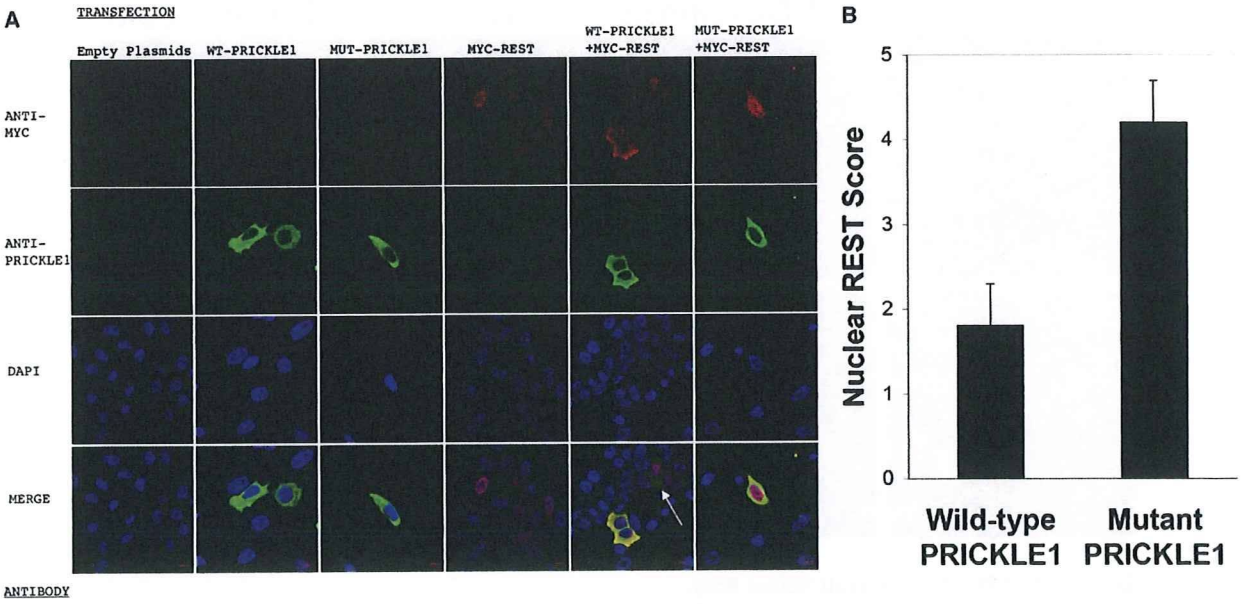

Figure 5. Subcellular Localization of Recombinant MYC-REST and WT or MUT PRICKLE1

(A) HeLa cells were transfected with MYC-REST and WT PRICKLE1 or MUT PRICKLE1, as noted on the top of the images in (A). Antibody staining with ANTI-MYC antibody (red), ANTI-PRICKLE1 antibody (green), DAPI nuclear staining (blue), and MERGED confocal images are noted on the left. Scale bar represents 9 microns. All confocal images were captured with identical exposure settings. The white arrow in the merged WT-PRICKLE1+MYC-REST marks a cell with relatively less WT PRICKLE1 expressed versus the two other WT PRICKLE1-expressing cells in the same panel. Note that increased REST in the nucleus is inversely proportional to WT PRICKLE1 expression, whereas the nuclear REST signal is strong even in the presence of a strong MUT PRICKLE1 signal (bottom right).

(B) Quantification of nuclear REST in PRICKLE1 versus mutant PRICKLE1 cotransfections. Results are the mean (±SD) of 100 cells for each group.

PRICKLE1 has also been implicated in the canonical WNT/β-catenin pathway.[25] Mutations in *EPM2A*, which cause Lafora disease—a severe form of PME with neurodegeneration—can affect the stability of the β-catenin complex in the canonical WNT/β-catenin pathway by dephosphorylating GSK3-β.[26] Although the involvement of PRICKLE1 and the influence of Epm2A on β-CATENIN may be unrelated, it is possible that a common pathway connects the effects of *PRICKLE1* mutations to Lafora disease and WNT signaling. It is notable that many affected

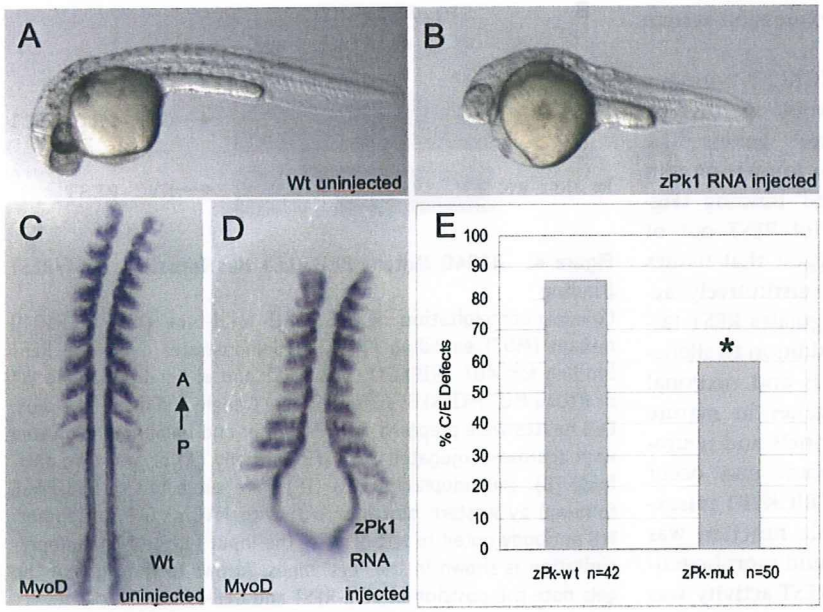

Figure 6. Mutant prickle1 Shows Decreased Activity In Vivo in Zebrafish

(A–D) Equivalent amounts of RNA encoding wild-type zebrafish *prickle1* (*pk*-wt) or zebrafish *prickle1* encoding the human R104Q homologous amino acid (*pk*-mut) were injected into zebrafish embryos and assayed for convergence extension defects by morphology (A) wild-type compared to (B) pk-overexpression, anterior to the left and with molecular markers to axial tissues in (C) wild-type and (D) pk-overexpressing embryos, anterior to the top.

(E) Decreased gastrulation defects are observed in mutant *prickle1* expressing embryos compared to wild-type *prickle* expressing embryos. The mutant Prickle1 showed significantly decreased overexpression phenotype, with a p value of 0.01 by the Fisher's exact test.

individuals with PME respond to medications such as valproic acid, which also affects the WNT/β-catenin signaling pathway through inhibition of GSK3-β.[27,28] On the other hand, valproic acid was also shown to alter inositol levels, which would interfere with calcium regulation.[29–31]

It is not yet clear how a mutation in human *PRICKLE1* leads to the PME syndrome, which is pathophysiologically characterized by increased cortical hyperexcitability with involvement of the cerebellum and probably other deep gray matter nuclei as well.

Future analysis of the effects of specific point mutations of *Prickle1* in animal models will further elucidate the molecular mechanisms underlying this PME-ataxia syndrome. Understanding the molecular and cellular basis of the disease may lead to improved diagnostic and therapeutic approaches for afflicted individuals.

Supplemental Data

Supplemental Data include one figure and two tables and can be found with this article online at http://www.ajhg.org/.

Acknowledgments

We thank the members of the families for their participation. We thank Chantal Allamargot and Kathy Walters for their assistance with immunostaining and confocal microscopy at the University of Iowa, and Kaye Suyama for her work with the antibodies at Stanford. A.G.B. is supported by NIH/NINDS grant K08NS48174. M.P.S. is an investigator of the Howard Hughes Medical Institute. D.C.S. and H.L.G. were supported by NIH CA112369. M.S. was supported by NIH/NCRR P20RR020171 and NIH MH067123. A.B. was supported by a grant from the Epilepsy Foundation. We thank Jeffrey Murray for access to the CEPH-HGD panel and for commentary on the manuscript. The authors have no disclosures and no conflicts of interest. A.G.B. wrote the manuscript, performed all immunohistochemical studies in HeLa cells and half of the tissue immunostaining, and oversaw all aspects of the resequencing, control genotyping, and coimmunoprecipitations. H.E. and A.D. clinically evaluated part of pedigree B. S.B. clinically evaluated all the pedigrees and integrated the clinical data, together with Z.A., S.K., A.K., M.N., S.W., A.Z., and R.S. H.E. and S.B. designed the mapping strategies. R.W., A.B., and S.C. performed the fine mapping, resequencing, and genotyping studies. A.B. compiled Table S1. S.C. compiled Table S2. A.R.B. performed the coimmunoprecipitations. P.F. and J.M. assisted in the design and analysis of he genotyping assays. M.N. ascertained and prepared the specimens for human tissue staining. S.W. prepared the Prickle1 antibody at the University of Iowa. P.G. assisted in the development of the cell-culture experiments. D.C.S. oversaw all zebrafish injections and analyses performed by H.L.G. M.S. provided the myc-REST construct and guidance in cell transfections. S.M. provided a mouse prickle1-GFP expression vector that was used in pilot studies in preparation for the use of a human Prickle1-EGFP construct. J.A., M.P.S., D.A., and E.K.V. produced the Prickle1 antibodies and performed the immunostaining at Stanford University.

Received: August 19, 2008
Revised: September 28, 2008
Accepted: October 3, 2008
Published online: October 30, 2008

Web Resources

The URLs for data presented herein are as follows:

Online Mendelian Inheritance in Man (OMIM), http://www.ncbi.nlm.nih.gov/Omim/
PHRAP, http://www.phroap.org

References

1. Berkovic, S.F., Mazarib, A., Walid, S., Neufeld, M.Y., Manelis, J., Nevo, Y., Korczyn, A.D., Yin, J., Xiong, L., Pandolfo, M., et al. (2005). A new clinical and molecular form of Unverricht-Lundborg disease localized by homozygosity mapping. Brain *128*, 652–658.
2. El-Shanti, H., Daoud, A., Sadoon, A.A., Leal, S.M., Chen, S., Lee, K., and Spiegel, R. (2006). A distinct autosomal recessive ataxia maps to chromosome 12 in an inbred family from Jordan. Brain Dev. *28*, 353–357.
3. Straussberg, R., Basel-Vanagaite, L., Kivity, S., Dabby, R., Cirak, S., Nurnberg, P., Voit, T., Mahajnah, M., Inbar, D., Saifi, G.M., et al. (2005). An autosomal recessive cerebellar ataxia syndrome with upward gaze palsy, neuropathy, and seizures. Neurology *64*, 142–144.
4. Ciani, L., and Salinas, P.C. (2005). WNTs in the vertebrate nervous system: from patterning to neuronal connectivity. Nat. Rev. Neurosci. *6*, 351–362.
5. Veeman, M.T., Axelrod, J.D., and Moon, R.T. (2003). A second canon. Functions and mechanisms of beta-catenin-independent Wnt signaling. Dev. Cell *5*, 367–377.
6. Carreira-Barbosa, F., Concha, M.L., Takeuchi, M., Ueno, N., Wilson, S.W., and Tada, M. (2003). Prickle 1 regulates cell movements during gastrulation and neuronal migration in zebrafish. Development *130*, 4037–4046.
7. Veeman, M.T., Slusarski, D.C., Kaykas, A., Louie, S.H., and Moon, R.T. (2003). Zebrafish prickle, a modulator of noncanonical Wnt/Fz signaling, regulates gastrulation movements. Curr. Biol. *13*, 680–685.
8. Takeuchi, M., Nakabayashi, J., Sakaguchi, T., Yamamoto, T.S., Takahashi, H., Takeda, H., and Ueno, N. (2003). The prickle-related gene in vertebrates is essential for gastrulation cell movements. Curr. Biol. *13*, 674–679.
9. Bastock, R., Strutt, H., and Strutt, D. (2003). Strabismus is asymmetrically localised and binds to Prickle and Dishevelled during *Drosophila* planar polarity patterning. Development *130*, 3007–3014.
10. Bellaiche, Y., Beaudoin-Massiani, O., Stuttem, I., and Schweisguth, F. (2004). The planar cell polarity protein Strabismus promotes Pins anterior localization during asymmetric division of sensory organ precursor cells in *Drosophila*. Development *131*, 469–478.
11. Tree, D.R., Shulman, J.M., Rousset, R., Scott, M.P., Gubb, D., and Axelrod, J.D. (2002). Prickle mediates feedback amplification to generate asymmetric planar cell polarity signaling. Cell *109*, 371–381.
12. Shimojo, M., and Hersh, L.B. (2003). REST/NRSF-interacting LIM domain protein, a putative nuclear translocation receptor. Mol. Cell. Biol. *23*, 9025–9031.
13. Shimojo, M., and Hersh, L.B. (2006). Characterization of the REST/NRSF-interacting LIM domain protein (RILP): localization and interaction with REST/NRSF. J. Neurochem. *96*, 1130–1138.

14. Galigniana, M.D., Radanyi, C., Renoir, J.M., Housley, P.R., and Pratt, W.B. (2001). Evidence that the peptidylprolyl isomerase domain of the hsp90-binding immunophilin FKBP52 is involved in both dynein interaction and glucocorticoid receptor movement to the nucleus. J. Biol. Chem. *276*, 14884–14889.
15. Gonzalez-Alegre, P., and Paulson, H.L. (2004). Aberrant cellular behavior of mutant torsinA implicates nuclear envelope dysfunction in DYT1 dystonia. J. Neurosci. *24*, 2593–2601.
16. Cann, H.M., de Toma, C., Cazes, L., Legrand, M.F., Morel, V., Piouffre, L., Bodmer, J., Bodmer, W.F., Bonne-Tamir, B., Cambon-Thomsen, A., et al. (2002). A human genome diversity cell line panel. Science *296*, 261–262.
17. Crompton, L.A., Du Roure, C., and Rodriguez, T.A. (2007). Early embryonic expression patterns of the mouse Flamingo and Prickle orthologues. Dev. Dyn. *236*, 3137–3143.
18. Katoh, M. (2003). Identification and characterization of human PRICKLE1 and PRICKLE2 genes as well as mouse Prickle1 and Prickle2 genes homologous to *Drosophila* tissue polarity gene prickle. Int. J. Mol. Med. *11*, 249–256.
19. Okuda, H., Miyata, S., Mori, Y., and Tohyama, M. (2007). Mouse Prickle1 and Prickle2 are expressed in postmitotic neurons and promote neurite outgrowth. FEBS Lett. *581*, 4754–4760.
20. Tissir, F., and Goffinet, A.M. (2006). Expression of planar cell polarity genes during development of the mouse CNS. Eur. J. Neurosci. *23*, 597–607.
21. Zuccato, C., Tartari, M., Crotti, A., Goffredo, D., Valenza, M., Conti, L., Cataudella, T., Leavitt, B.R., Hayden, M.R., Timmusk, T., et al. (2003). Huntingtin interacts with REST/NRSF to modulate the transcription of NRSE-controlled neuronal genes. Nat. Genet. *35*, 76–83.
22. Palm, K., Belluardo, N., Metsis, M., and Timmusk, T. (1998). Neuronal expression of zinc finger transcription factor REST/NRSF/XBR gene. J. Neurosci. *18*, 1280–1296.
23. Ciruna, B., Jenny, A., Lee, D., Mlodzik, M., and Schier, A.F. (2006). Planar cell polarity signalling couples cell division and morphogenesis during neurulation. Nature *439*, 220–224.
24. Olguin, P., Oteiza, P., Gamboa, E., Gomez-Skarmeta, J.L., and Kukuljan, M. (2006). RE-1 silencer of transcription/neural restrictive silencer factor modulates ectodermal patterning during *Xenopus* development. J. Neurosci. *26*, 2820–2829.
25. Chan, D.W., Chan, C.Y., Yam, J.W., Ching, Y.P., and Ng, I.O. (2006). Prickle-1 negatively regulates Wnt/beta-catenin pathway by promoting Dishevelled ubiquitination/degradation in liver cancer. Gastroenterology *131*, 1218–1227.
26. Liu, Y., Wang, Y., Wu, C., and Zheng, P. (2006). Dimerization of Laforin is required for its optimal phosphatase activity, regulation of GSK3beta phosphorylation, and Wnt signaling. J. Biol. Chem. *281*, 34768–34774.
27. Chen, G., Huang, L.D., Jiang, Y.M., and Manji, H.K. (1999). The mood-stabilizing agent valproate inhibits the activity of glycogen synthase kinase-3. J. Neurochem. *72*, 1327–1330.
28. Wiltse, J. (2005). Mode of action: inhibition of histone deacetylase, altering WNT-dependent gene expression, and regulation of beta-catenin–developmental effects of valproic acid. Crit. Rev. Toxicol. *35*, 727–738.
29. Galit, S., Shirley, M., Ora, K., Belmaker, R.H., and Galila, A. (2007). Effect of valproate derivatives on human brain myo-inositol-1-phosphate (MIP) synthase activity and amphetamine-induced rearing. Pharmacol. Rep. *59*, 402–407.
30. Shimshoni, J.A., Dalton, E.C., Jenkins, A., Eyal, S., Ewan, K., Williams, R.S., Pessah, N., Yagen, B., Harwood, A.J., and Bialer, M. (2007). The effects of central nervous system-active valproic acid constitutional isomers, cyclopropyl analogs, and amide derivatives on neuronal growth cone behavior. Mol. Pharmacol. *71*, 884–892.
31. Tokuoka, S.M., Saiardi, A., and Nurrish, S.J. (2008). The mood stabilizer valproate inhibits both inositol- and diacylglycerol-signaling pathways in *Caenorhabditis elegans*. Mol. Biol. Cell *19*, 2241–2250.

Neuroscience Letters 445 (2008) 162–165

Contents lists available at ScienceDirect

Neuroscience Letters

journal homepage: www.elsevier.com/locate/neulet

PRMT1 and Btg2 regulates neurite outgrowth of Neuro2a cells

Shingo Miyata[a,b,*], Yasutake Mori[a], Masaya Tohyama[a,b]

[a] Department of Anatomy and Neuroscience, Graduate School of Medicine, Osaka University, 2-2 Yamadaoka, Suita, Osaka 565-0871, Japan
[b] Department of Clinical Disorder Research, The Osaka-Hamamatsu Joint Research Center For Child Mental Development, 2-2 Yamadaoka, Suita, Osaka 565-0871, Japan

ARTICLE INFO

Article history:
Received 26 June 2008
Received in revised form 15 August 2008
Accepted 19 August 2008

Keywords:
PRMT1
Btg2
Neurite outgrowth
Neuro2a cells
Arginine methylation

ABSTRACT

Neurite outgrowth is one of the crucial events in the formation of neural circuits. The majority of studies on neurite outgrowth have focused on signal transduction processes based on phosphorylation and acetylation; a few studies have suggested the involvement of other molecular mechanisms. Recent progress in understanding the nature of protein arginine *N*-methyltransferases (PRMTs) raises the possibility of the involvement of protein methylation accompanied by cell shape changes during neuronal differentiation. Here, we show that PRMT1 play a pivotal role in the neurite outgrowth of Neuro2a cells. Our results revealed that PRMT1 depletion specifically affected neurite outgrowth but not the physiological processes involved in cell growth and differentiation. Furthermore, we demonstrated that Btg2, one of the PRMT1 binding partner, depletion down-regulated arginine methylation in the nucleus and inhibited neurite outgrowth. These results indicate that protein arginine methylation by PRMT1 in the nucleus is an important step in neuritogenesis.

Neurite outgrowth is extremely important for the formation of neural circuits during the developmental stage, and the reformation of neurite outgrowth plays an essential role in intractable neurodegenerative disorders [9,15]. Furthermore, most studies on neurite outgrowth have focused on signal transduction processes such as phosphorylation and acetylation [7,11,12,16]. Although the functional significance of protein methylation in nonneuronal cells has been proposed [1,2,19,18,21], its significance in neuronal cells is unknown. Recently, several studies indicated that the function of protein methylation in neuron-like cells is that arginine *N*-methylation that may cause neurite outgrowth [4–6]; however the molecular mechanism underlying this process remains unclear.

It is known that the Btg2 protein can bind to PRMT1 and increasing PRMT1 activity [14]. Furthermore, it has been reported that Btg2 is related to neuronal differentiation [8]. In this study, we demonstrate that PRMT1 is necessary for neurite outgrowth, and Btg2 expression may regulate protein arginine methylation by PRMT1 in the nucleus of Neuro2a cells by using the transient PRMT1 depletion method.

Neuro2a cells (IF050081) were obtained from the Human Science Research Resources Bank (HSRRB). These cells were maintained in Dulbecco's modified Eagle's medium (DMEM) (Invitrogen Co.) containing 10% heat-inactivated fetal bovine serum (FBS) at 37 °C in an atmosphere of 95% air/5% CO_2. For the neurite outgrowth studies, Neuro2a cells (5×10^5 cells) were cultured in DMEM containing 0.1% bovine serum albumin (BSA). When cells attained a length greater than two cell diameters they were scored for the production of outgrowths. The number of neurite-bearing cells was expressed as a percentage of the total cell number (>50 μm; three independent experiments, 300 cells each).

In order to investigate the functions of well-studied protein arginine methyltransferase, PRMT1, on the neurite outgrowth of Neuro2a cells, we first examined the effects of PRMT1 depletion from the cells by an RNA interference (RNAi)-based knockdown method. Stealth siRNA against PRMT1 (5′-AUAGGAGUCAAAGUAGUAGUCUUUG-3′), and negative control duplexes (scrambled siRNA for PRMT1, 5′-CAAAUCACAUCGUUUCUCACGAUAU-3′) were provided by Invitrogen Co. The Neuro2a cells were transfected with 100 pM of each siRNA and a mixture of scrambled siRNA by using Lipofectamine RNAiMAX (Invitrogen Co.) according to the manufacturer's instructions. Western blot analysis also demonstrated that the expression of endogenous PRMT1 in Neuro2a cells was extinguished by the PRMT1 siRNA (Fig. 1A). PRMT1-targeted siRNA significantly reduced the endogenous PRMT1 level with almost no effect on the CARM1 level (PRMT1 and CARM1 antibodies, 1:1000; Upstate Biotech) (PRMT1, 0.13 ± 0.18; CARM1, 0.98 ± 0.05) (Fig. 1A). Similarly, previous studies demonstrated that PRMT1-

Abbreviations: Btg2, B-cell translocation gene 2; BSA, bovine serum albumin; FBS, fetal bovine serum; NGF, nerve growth factor; PRMT1, protein arginine *N*-methyltransferase 1; siRNA, small interfering RNA; YFP, yellow fluorescent protein.

* Corresponding author at: Department of Anatomy and Neuroscience, Graduate School of Medicine, Osaka University, 2-2 Yamadaoka, Suita, Osaka 565-0871, Japan.
E-mail address: smiyata@anat2.med.osaka-u.ac.jp (S. Miyata).

0304-3940/$ – see front matter © 2008 Elsevier Ireland Ltd. All rights reserved.
doi:10.1016/j.neulet.2008.08.065

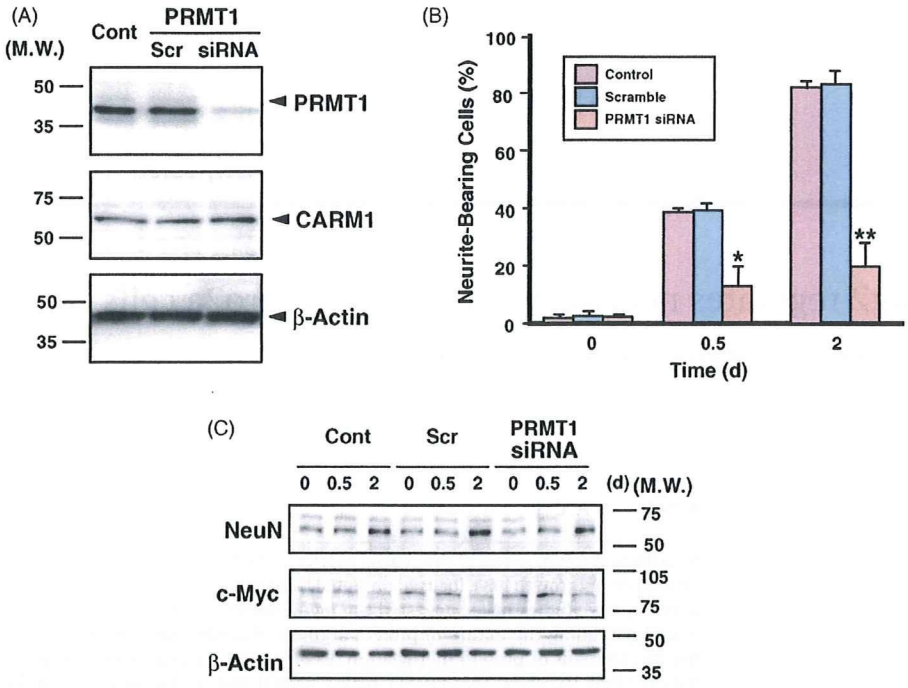

Fig. 1. Effects of PRMT1 knockdown on neurite outgrowth and differentiated neuronal phenotypes of Neuro2a cells. (A) Data representing the western blot analysis of PRMT1, CARM1, and β-actin protein expression 3 days after transfection with scrambled, or PRMT1-siRNA. Cont, nontransfected cells; Scr, scrambled siRNA-transfected cells. M.W., molecular weight. (B) Quantification of the neurite outgrowth levels of the PRMT1 depletion Neuro2a cells. The results are expressed as the mean ± S.E.M. of three independent experiments. The asterisks (*) indicate the significant effects of a decrease in the number of neurite-bearing cells (Student's *t*-test; $^{*}P < 0.05$, $^{**}P < 0.01$). (C) Changes in the expression levels of the neuronal marker NeuN and the cell proliferation markers c-Myc in the PRMT1 siRNA-transfected cells after serum withdrawal. The total cell lysate was subjected to western blot analysis by using the anti-NeuN, anti-c-Myc, or anti-β-actin antibodies. M.W., molecular weight; d, days.

targeted siRNA specifically reduced endogenous PRMT1 expression to 10–20% [10,13]. Therefore, the employed sequence of double-stranded siRNA effectively suppressed the expression of the PRMT1 genes in Neuro2a cells.

To elucidate a functional significance of protein arginine methylation, we examined the effect of PRMT1 depletion on the neuritogenesis of Neuro2a cells induced by serum deprivation. Three days after Neuro2a cells were transfected with scrambled or PRMT1-targeted siRNA were counted as neurite-bearing cells (Fig. 1B). In the growth media containing 10% fetal bovine serum , the scrambled, PRMT1-targeted siRNAs did not induce neurite outgrowth 2 days after the transfection (data not shown). Serum deprivation caused significant neurite outgrowth in the scrambled siRNA-transfected group (data not shown), while transfection with PRMT1-targeted siRNA reduced the neurite-bearing population to 20% of that observed with transfection with scrambled siRNA under the same condition (scrambled siRNA, 85.3% ± 5.2%; PRMT1 siRNA, 21.7% ± 8.6%) (Fig. 1B).

The immunodetection was performed using the ECL Western blotting detection system (GE Healthcare Bio-Science) with peroxidase-coupled secondary antibody according to the manufacturer's instructions. Interestingly enough, this siRNA-transfected cells showed an enhancement in the neuronal marker protein NeuN (1:1000; Chemicon International Inc.) 2 days after serum deprivation, while c-Myc (1:1000; Sigma–Aldrich), a proliferating marker protein, was gradually reduced (Fig. 1C). These results demonstrated that PRMT1 depletion specifically affected neurite outgrowth but not the physiological processes involved in cell growth and differentiation.

To confirm whether the reintroduction of PRMT1 into its siRNA-transfected cells reverted the knockdown phenotype, 3 days after the scrambled or PRMT1 siRNA transfection, a PRMT1 construct harboring some neutral mutations along the siRNA oligonucleotide sequence was retransfected into the Neuro2a cells. The siRNA-resistant mutant PRMT1 was visualized by the fused yellow fluorescent protein (YFP) in its N-terminus. We performed a western blot analysis and immunocytochemistry of the YFP-fused siRNA-resistant mutant PRMT1 protein expression. This fusion protein and mock YFP proteins were transiently expressed in Neuro2a cells (Fig. 2A and B), and the anti-GFP polyclonal antibody (1:1000; Abcam Ltd.) recognized either of the two proteins with expected sizes of 25 and 65 kDa, respectively (Fig. 2D). Furthermore, the anti-PRMT1 polyclonal antibody recognized only the YFP-fused siRNA-resistant mutant PRMT1 protein (Fig. 2D). Thus, we used this fusion protein to perform the subsequent experiments. The overexpressed mutant PRMT1 in the siRNA-transfected cells elevated the population of neurite-bearing cells by 2.5-fold compared to the control YFP protein (cells cultured for 2 days in the differentiation medium; YFP, 12.2% ± 2.3%; YFP-fused PRMT1, 28.2% ± 5.3%) (Fig. 2C). These findings demonstrated that arginine methylation induced by the PRMT1 protein was deeply linked to the neurite outgrowth of Neuro2a cells.

Since Btg2 was reported to be one of the interacting partners screened by the two-hybrid method using PRMT1 as bait [14], we examined the effects of the depletion of Btg2 from Neuro2a cells on the level of methylated proteins and neurite extension. Stealth siRNA against Btg2 (5′-UGUAAUGAUCGGUCAGUGCGUCCUG-3′) and negative control duplexes (scrambled siRNA for Btg2, 5′-CAGCGCACUGACCGAUCAUUGAACA-3′) were provided by Invitrogen Co. Real-time PCR was performed on an ABI PRISM 7900HT Sequence Detection System using the SYBR GREEN PCR Master Mix (Applied Biosystems). To quantify Btg2 expression levels the following primers were used: forward, 5′-ATGAGCCACGGGAAGAGAAC-3′; reverse, 5′-

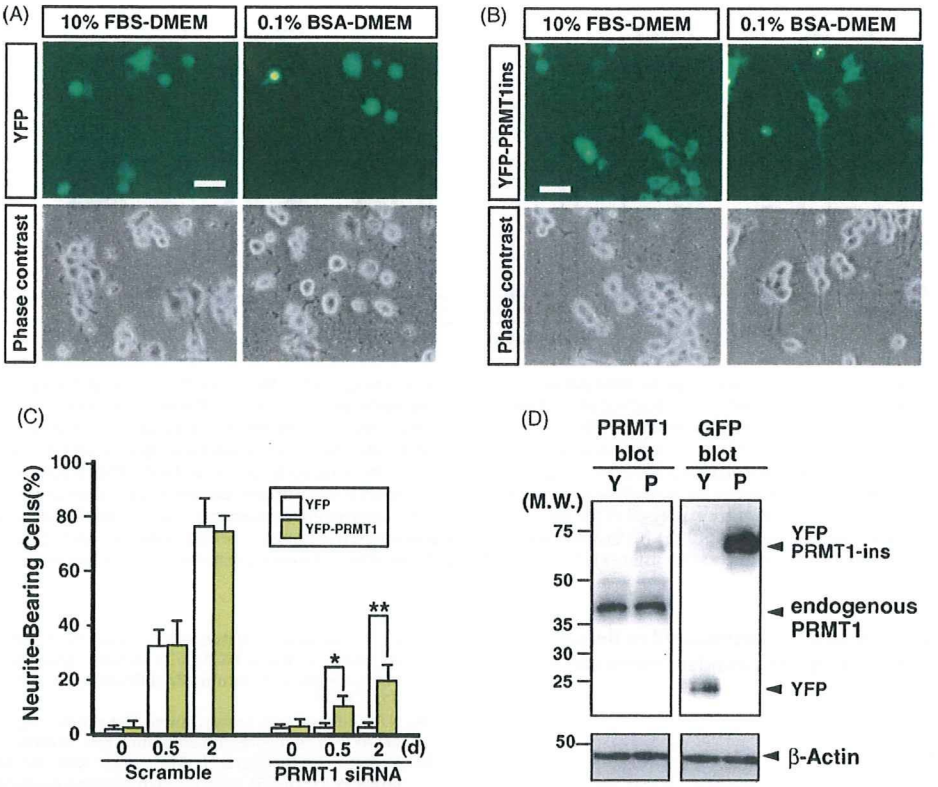

Fig. 2. PRMT1 expression necessary for the neurite outgrowth of Neuro2a cells. (A and B) Fluorescent micrographs of the Neuro2a cells. Depletion of PRMT1 in Neuro2a cells by transfection with 100 pM PRMT1 siRNA and mock YFP (A) or YFP-fused siRNA insensitive PRMT1 (B) for 3 days is shown. Cells were grown in normal growth medium (10% FBS) or differentiation medium (0.1% BSA) for 2 days. Bar, 30 μm. (C) Quantification of the results shown in panel A and B. PRMT1 expression is necessary for neurite outgrowth in the Neuro2a cells. PRMT1 siRNA-insensitive, YFP-fused PRMT1 (yellow) or mock YFP (white) expressed in PRMT1-depleted Neuro2a cells cultured for 2 days. The results are expressed as the mean ± S.E.M. of three independent experiments. The asterisks indicate the significant effects of an increase in the number of neurite-bearing cells (Student's *t*-test; $^{*}P < 0.05$, $^{**}P < 0.01$). (D) Checking the expression of YFP-fused siRNA-insensitive PRMT1 in Neuro2a cells. Y, mock YFP-transfected cell lysate; P, YFP-fused siRNA insensitive PRMT1-transfected cell lysate; M.W., molecular weight.

GCTGGAGACGGCCATCACAT-3′. As primers for ribosomal protein L27 (RPL27) primers: forward, 5′-TGTGTGGATATCCCCTTGGA-3′; reverse, 5′-TAAAAGCGAAGCTTCTGGAAA-3′. The fluorescence derived from the incorporation of SYBR Green I into the double-stranded PCR products was performed and measured according to the manufacturer's instructions (Applied Biosystems). In Btg2-targeted siRNA-transfected cells, the optimal induction of Btg2 mRNA after serum withdrawal was reduced to 20% of that in the scrambled siRNA-transfected cells (Fig. 3A), with almost no effect on PRMT1 and CARM1 protein expression (data not shown). At the same time point, the nuclear fractions of the Btg2 siRNA-transfected cells exhibited a significant decrease in the level of arginine-methylated proteins recognized by the ASYM24 antibody (1:500; Upstate Biotech) (scrambled siRNA, 1.00 ± 0.53; Btg2 siRNA, 0.58 ± 0.10) (Fig. 3B). However, the cytoplasmic fraction of the Btg2 siRNA-transfected cells did not show any change in the arginine-methylated protein level (scrambled siRNA, 1.00 ± 0.41; Btg2 siRNA, 1.12 ± 0.79) (Fig. 3B). These results showed that Btg2 might act as one of the regulators of arginine-methylating activity in the nuclear fraction possibly though interaction with PRMT1. Furthermore, the Btg2-targeted siRNA decreased the population of neurite-bearing cells 2 days after serum deprivation (2 days: scrambled siRNA, 78.2% ± 8.3%; Btg2 siRNA, 32.4% ± 9.3%) (Fig. 3C). These results raised the possibility that Btg2 expression was one of the regulators of PRMT1 activity in the nucleus through the neurite outgrowth of Neuro2a cells.

The recent investigations and functional analyses of the PRMT family raised the possibility that protein arginine methylation is highly regulated in response to external stimuli and may play different roles in physiological processes; however the functions of the PRMT family in the nervous system remain unknown [3,17]. This report demonstrated that the neurite outgrowth of Neuro2a cells might be regulated by the PRMT1 and Btg2 expressions. This result is in keeping with that of a previous report on the drug-induced inhibition of the protein methylation of PC12 cells that caused the loss of neurite extension in the presence of NGF with no effect on the survival rate [5]. The recovery of YFP-fused PRMT1 in the knockdown cells partly reverted the defective neuritogenesis in the serum-starved condition (Fig. 2), confirming that the knockdown phenotype was attributable to the loss of PRMT1. In this study, we further demonstrated that the Btg2 expression is related to neurite outgrowth (Fig. 3). These results indicate that one of the possible mechanisms of neurite outgrowth is regulated by Btg2 protein induction and PRMT1 activity regulation. It is well known that many RNA-binding proteins modify arginine methylation [20] and that the Btg2 protein can bind to PRMT1, thereby increasing PRMT1 activity [14]. This suggests that the expression of Btg2 and up-regulate PRMT1 activity plays an important role in the function of RNA-binding proteins in arginine methylation and can change the localization of specific mRNAs in neurons; this confirms the fact that arginine methylation is an important event in the formation of neural circuits. Therefore, it is likely that arginine methylation is emerging as a major regulator of protein function.

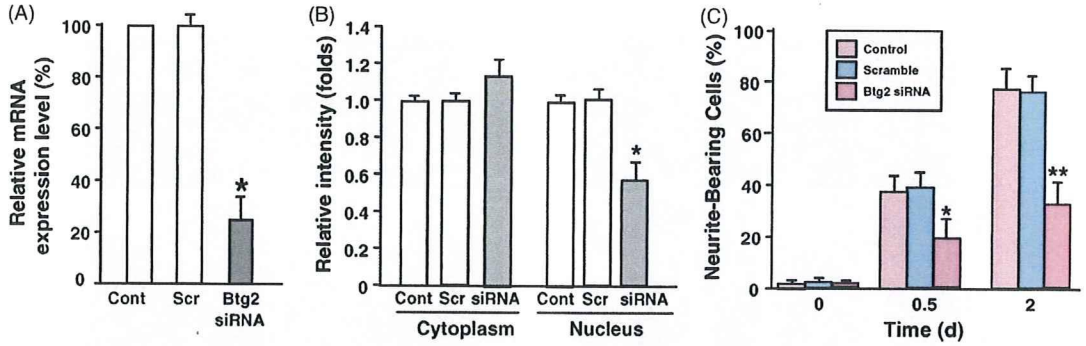

Fig. 3. Knockdown of Btg2 mRNA expression decreases arginine methylation and inhibits neurite outgrowth in Neuro2a cells. Real-time PCR analysis of Btg2 mRNA expressi in Neuro2a cells transfected with 200 pM scrambled (Scr) or Btg2 siRNA for 3 days or in a nontransfected control (Cont). The results are expressed as the mean ± S.E.M. of thr independent experiments. The asterisks (*) indicate the significant effects of a decrease in Btg2 mRNA expression after Btg2 siRNA transfection ($P < 0.05$). (B) Quantificati of the results of the siRNA-transfected Neuro2a cells were fractionated into cytoplasmic and nuclear fractions that were analyzed by western blotting with the anti-ASYM antibody. As controls, Neuro2a cell lysates were analyzed using an anti-β-actin and anti-histonH4 antibody. Scr, scrambled siRNA-transfected cells; siRNA, Btg2 siRN transfected cells. The data are presented as relative to the level of the expression of every asymmetric dimethylated protein in the lysates of nontransfected cells detected the ASYM24 antibody at 0 h (set at 1.0). The results are expressed as the mean ± S.E.M. of three independent experiments. The asterisk (*) indicates the significant effects c decrease in the relative intensities (Student's *t*-test; $^*P < 0.05$). (C) Quantification of the neurite outgrowth levels of the Btg2 depletion Neuro2a cells. The results are express as the mean ± S.E.M. of three independent experiments. The asterisks (*) indicate the significant effects of a decrease in the number of neurite-bearing cells (Student's *t*-te $^*P < 0.05$, $^{**}P < 0.01$).

It is possible that the examination of methylated or demethylated RNA-binding proteins will clarify the candidate molecular mechanisms of neuritogenesis.

Acknowledgements

We greatly thank Ms. A. Arakawa, Ms. Y. Ohashi and Ms. E. Moriya for technical assistances. This work was, in part, supported by the Osaka Medical Research Foundation for Incurable Diseases, Grant-in-Aid for Scientific Research (No. 20700335) from Japan Society for the Promotion of Science, and the 21st Century COE Program from the Ministry of Education, Culture, Sports, Science, and Technology of Japan.

References

[1] C. Abramovich, B. Yakobson, J. Chebath, M. Revel, A protein-arginine methyltransferase binds to the intracytoplasmic domain of the IFNAR1 chain in the type I interferon receptor, EMBO J. 16 (1997) 260–266.
[2] A.J. Bannister, T. Kouzarides, Reversing histone methylation, Nature 436 (2005) 1103–1106.
[3] M.T. Bedford, S. Richard, Arginine methylation: an emerging regulator of protein function, Mol. Cell 18 (2005) 263–272.
[4] B. Birkaya, J.M. Aletta, NGF promotes copper accumulation required for optimum neurite outgrowth and protein methylation, J. Neurobiol. 63 (2005) 49–61.
[5] T.R. Cimato, J.E. Murray, X. Zhou, J.M. Aletta, Nerve growth factor-specific regulation of protein methylation during neuronal differentiation of PC12 cells, J. Cell Biol. 138 (1997) 1089–1103.
[6] T.R. Cimato, J. Tang, Y. Xu, C. Guarnaccia, H.R. Herschman, S. Pongor, J.M. Aletta, Nerve growth factor-mediated increases in protein methylation occur predominantly at type I arginine methylation sites and involve protein arginine methyltransferase I, J. Neurosci. Res. 67 (2002) 435–442.
[7] R.J. Davis, Signal transduction by the JNK group of MAP kinases, Cell 103 (2000) 239–252.
[8] F. El-Ghissassi, S. Valsesia-Wittmann, N. Falette, C. Duriez, P.D. Wald A. Puisieux, BTG2(TIS21/PC3) induces neuronal differentiation and p vents apoptosis of terminally differentiated PC12 cells, Oncogene 21 (20 6772–6778.
[9] N.O. Glebova, D.D. Ginty, Growth and survival signals controlling sympathe nervous system development, Annu. Rev. Neurosci. 28 (2005) 191–222.
[10] K. Hata, K. Nishijima, J. Mizuguchi, Role for Btg1 and Btg2 in grov arrest of WEHI-231 cells through arginine methylation following membr immunoglobulin engagement, Exp. Cell Res. 313 (2007) 2356–2366.
[11] E.J. Huang, L.F. Reichardt, Trk receptors: roles in neuronal signal transducti Annu. Rev. Biochem. 72 (2003) 609–642.
[12] A. Hudmon, H. Schulman, Neuronal CA2+/calmodulin-dependent prot kinase. II. The role of structure and autoregulation in cellular function, An Rev. Biochem. 71 (2001) 473–510.
[13] M.A. Kleinschmidt, G. Streubel, B. Samans, M. Krause, U.M. Bauer, The prot arginine methyltransferases CARM1 and PRMT1 cooperate in gene regulati Nucleic Acids Res. 36 (2008) 3202–3213.
[14] W.J. Lin, J.D. Gary, M.C. Yang, S. Clarke, H.R. Herschman, The mammal immediate-early TIS21 protein and the leukemia-associated BTG1 prot interact with a protein-arginine *N*-methyltransferase, J. Biol. Chem. 271 (19 15034–15044.
[15] L. Luo, D.D. O'Leary, Axon retraction and degeneration in development disease, Annu. Rev. Neurosci. 28 (2005) 127–156.
[16] B. Mayr, M. Montminy, Transcriptional regulation by the phosphorylati dependent factor CREB, Nat. Rev. Mol. Cell Biol. 2 (2001) 599–609.
[17] A.E. McBride, P.A. Silver, State of the arg: protein methylation at arginine cor of age, Cell 106 (2001) 5–8.
[18] D. Passeri, A. Marcucci, G. Rizzo, M. Billi, M. Panigada, L. Leonardi, F. Tiron Grignani, Btg2 enhances retinoic acid-induced differentiation by modulat histone H4 methylation and acetylation, Mol. Cell Biol. 26 (2006) 5023–50
[19] J. Tang, P.J. Kao, H.R. Herschman, Protein-arginine methyltransferase I, predominant protein-arginine methyltransferase in cells, interact with an regulated by interleukin enhancer-binding factor 3, J. Biol. Chem. 275 (20 19866–19876.
[20] E. Tran, J. Brown, E.S. Maxwell, Evolutionary origins of the RNA-gui nucleotide-modification complexes: from the primitive translation apparat Trends Biochem. Sci. 29 (2004) 343–350.
[21] V.L. Tybulewicz, Vav-family proteins in T-cell signaling, Curr. Opin. Immu 17 (2005) 267–274.